



Evaluation of target volume and dose accuracy in intrafractional cases of lung cancer based on 4D-CT and 4D-CBCT images using an in-house dynamic thorax phantom

Firyal Dhiyaul Haqqi¹, Arief Sudarmaji¹, Wahyu Edy Wibowo², Nuruddin Nasution², Handoko Handoko², Annisa Rahma Fauzia², Jihadil Qudsi³, Supriyanto Ardjo Pawiro¹

¹Department of Physics, Faculty of Mathematics and Natural Sciences, Universitas Indonesia, Depok, West Java, Indonesia

²Department of Radiation Oncology, Faculty of Medicine, Universitas Indonesia, dr. Cipto Mangunkusumo General Hospital, Jakarta, Indonesia

³Department of Medical Record and Medical Informatics, Politeknik Medica Farma Husada, Mataram, West Nusa Tenggara, Indonesia

ABSTRACT

Background: This study aimed to evaluate the target volume and dose accuracy in intrafraction cases using 4-dimensional imaging modalities and an in-house dynamic thorax phantom. Intrafraction motion can create errors in the definition of target volumes, which can significantly affect the accuracy of radiation delivery. Motion management using 4-dimensional modalities is required to reduce the risk.

Materials and methods: Two variations in both breathing amplitude and target size were applied in this study. From these variations, internal target volume (ITVs) contoured in 10 phases of 4D-CT (ITV₁₀), average intensity projection (AIP), and mid-ventilation (Mid-V) images were reconstructed from all 4D-CT datasets as reference images. Free-breathing (FB), augmentation free-breathing (Aug-FB), and static images were also acquired using the 3D-CT protocol for comparisons. In dose evaluations, the 4D-CBCT modality was applied before irradiation to obtain position correction. Then, the dose was evaluated with Gafchromic film EBT3.

Results: The ITV₁₀, AIP, and Mid-V provide GTVs that match the static GTV. The AIP and Mid-V reference images allowed reductions in ITVs and PTVs without reducing the range of target movement areas compared to FB and Aug-FB images with varying percentages in the range of 29.17% to 48.70%. In the dose evaluation, the largest discrepancies between the measured and planned doses were 10.39% for the FB images and 9.21% for the Aug-FB images.

Conclusion: The 4D-CT modality can enable accurate definition of the target volume and reduce the PTV. Furthermore, 4D-CBCT provides localization images during registration to facilitate position correction and accurate dose delivery.

Key words: 4D-CT; 4D-CBCT; dose evaluation; in-house phantom; volume evaluation

Rep Pract Oncol Radiother 2022;27(2):360-370

Introduction

Intrafractional motion of tumours induced by human respiration is a prominent source of un-

certainties in radiation therapy for lung cancer. Steven et al. stated that the mean tumour motion of the 22 patients studied was 4.5 ± 5 mm, and 12 of the 22 patients had a mean tumour motion in

Address for correspondence: Supriyanto Ardjo Pawiro, Department of Physics, Faculty of Mathematics and Natural Sciences, Universitas Indonesia, tel: +62-21-7872610; e-mail: supriyanto.p@sci.ui.ac.id

This article is available in open access under Creative Common Attribution-Non-Commercial-No Derivatives 4.0 International (CC BY-NC-ND 4.0) license, allowing to download articles and share them with others as long as they credit the authors and the publisher, but without permission to change them in any way or use them commercially

the SI direction of 8.3 ± 3.7 mm [1]. In another research, Huang et al., in their study of 7 lung cancer patients, found that lung tumours rotated at an angle of more than 5° in the SI direction [2]. Such motion has been a crucial challenge for medical physicists due to its impact on target definition, the setup position of the patient, and dose delivery [3]. According to the ICRU Report 62, the motion of a tumour is considered by including an internal margin around the clinical target volume (CTV) to establish the internal target volume (ITV). Nevertheless, the scheme has limitations, especially for tumours with significant movement. The addition of margins generates several irradiated healthy tissue volumes, consequently increasing the complication risk and reducing the possibility of dose escalation [4].

Computed tomography (CT) imaging correlated with breathing movement (4D-CT) is considered a method of choice for capturing moving targets. The accuracy of defining the target volume determines treatment success [5]. 4D-CT diminishes movement artefacts for precise target volume definition and concurrently permits patient-individual motion evaluation for safety margins [6]. Respiratory management using 4D-CT combined with 4D Image Guidance can reduce, at least 37% of the target volume compared to 3D-CT combined with 3D Image Guidance [7].

A significant indication suggests that 4D-CT scales down motion artefacts and renders localization of the target more convincing than 3D-CT. Nevertheless, 3D-CT has a concept to manage the target motion by using the augmentation free-breathing (Aug-FB) technique. This technique adds images at peak inhalation and peak expiration conditions to create ITV around its blurred GTV [8]. In several investigation, 4D-CT provides better target coverage and shrinks the area of healthy tissue irradiation during treatment for selected cases, especially tumour in the base of lung [9]. The ITV_{10} -based concept, which delineates a tumour in every single respiration phase, is commonly implemented and considers all cycles of motion, thus ensuring sufficient tumour coverage, although a larger part of the healthy lung is ultimately irradiated. The other concept is to define the tumour volume on a single phase, which is the phase closest to the time-weighted geometric centre of movement or the mid-ventilation phase (Mid-V). Thomas et al.

[10] suggest planning on a Mid-V image because the image can reduce the target volume and allow more accurate definition of the GTV. Several studies have conducted planning and dose calculations using average intensity projection (AIP) images [5, 11].

Tumour motion potentially leads to a difference between the planned dose and delivered dose due to setup errors [5]. Therefore, breathing-correlated 4D-CT must be unified into a 4D-IG workflow. Image guidance is the crucial stage in the radiotherapy treatment sequence to improve the accuracy of lung cancer treatment. 4D-CBCT is one of several methods for implementing 4D-IG [12]. At the image registration stage in the image guidance workflow, the 4D-CBCT modality provides better accuracy to reduce differences in target volume localization between planning and treatment [13]. The image-guided strategy is playing an increasingly important role in the development of radiotherapy in a more adaptive direction, not only in the patient setup but also in monitoring the dose delivered; therefore, this strategy can confer accuracy and confidence when performing dose escalation and provide more opportunities to implement the stereotactic body radiation therapy (SBRT) technique in lung cancer radiation treatment [14].

Aim

This study was designed to compare the target volume contouring and dose accuracy of five types of CT imaging [ITV_{10} , AIP, Mid-V, free-breathing (FB), and augmentation-free breathing (Aug-FB)] using an in-house dynamic thorax phantom.

Materials and methods

In-house dynamic thorax phantom development

As shown in Figure 1A, a dynamic thorax phantom was designed and created to be a quality control tool of tumour motion in the thoracic region by evaluating the geometry and dose accuracy. Several groups have investigated dose delivery accuracy in phantom studies. Mohatt et al. evaluated the combination of imaging techniques which is obtained from 4D dataset and computational algorithms best compensates for dosimetric accuracy on moving target using Quasar dynamic phantom [15]. Dai et al. in their investigation had done 3D dose verifica-

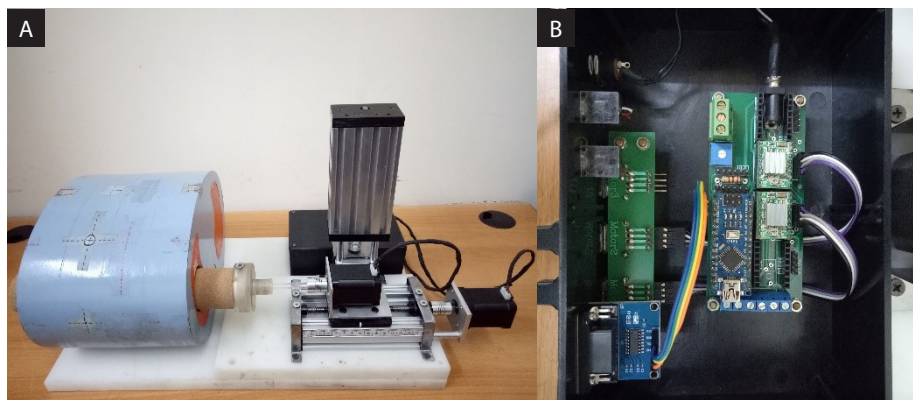


Figure 1. A. Assembly of the in-house dynamic thorax phantom; B. Controller of the dynamic component

tion for time dependant lung target displacement with Electromagnetic Tracking (EMT) system and 4D-CBCT using CIRS phantom [16]. In this study, in-house dynamic phantom was schemed based on the clinical investigations mentioned in the background, the phantom was designed to be able to mimic breathing-induced tumour movement with several variations in peak-to-peak amplitude ranging from 4.99 ± 0.04 mm to 29.61 ± 0.22 mm in the superior-inferior direction and angle variations in rotational movement ranging from 0 to $90.2 \pm 0.22^\circ$ in a sinusoidal waveform. The dynamic phantom can also provide several respiration rate options including 9, 14, and 27 rpm (respirations per minute). The body of the phantom is composed of local materials; acrylic ($\rho = 1.10$ g/cm³) is the soft tissue surrogate, and cork ($\rho = 0.22$ g/cm³) and teflon ($\rho = 1.88$ g/cm³) replicate lung and bone, respectively. The spherical target was composed of acrylic with diameters of 2 cm and 3 cm. The dynamic component of the phantom, as the target holder, was designed and controlled by stepper motors and ATmega328 (Arduino Nano 3.x) (Fig. 1B).

In this study, two target diameter variations were applied with 5-mm and 10-mm amplitudes in the SI direction and an 8° angle for rotational motion. The respiration rate used in this study was 14 rpm. It is selected based on the normal human respiratory rate, ranging from 12 to 20 respirations/minute [17].

Reference image acquisition and reconstruction

As reference images, 4D-CT images were acquired on a 64-slice CT simulator, the SOMATOM

Confidence RT Pro (Siemens Healthcare GmbH, Germany), for breathing-correlated CT. The respiration waveform representing the respiration state was detected by an Anzai AZ733 V pressure sensor (Anzai Medical Co., Japan). Image acquisition was carried out using two protocols: a 3D protocol and 4D protocol. The scanning parameters for the 4D protocol were 120 kV, 70 mAs, pitch 0.09, slice thickness 2.0 mm, a field of view (FOV) of 650×650 mm, and the use of a retrospective method with axial cine scanning. CT images of all breathing phases were obtained, transferred to a workstation and sorted retrospectively into ten phases (0–90%) by phase-binning algorithms, with 0% corresponding to peak inhalation and 50% corresponding to peak exhalation.

In addition, to consider the absence of 4D-CT in clinical situations, 3D image acquisition was also performed for comparison. The 3D image acquisition parameters were 120 kV, 77 mAs, pitch 0.35, number of slices 101, slice thickness 2.0 mm, and scanning in helical mode. In this protocol, three acquisition techniques were performed: static, FB, and Aug-FB. Three types of images were obtained with Aug-FB: images while moving and free-breathing, images at peak inspiration, and images at peak expiration.

All CT datasets obtained with both the 3D and 4D protocols were then transferred to the Syngovia Workstation (Syngovia, Siemens Medical Solutions, Forchheim, Germany). Furthermore, AIP images were reconstructed, and Mid-V images were also identified from 10 phases in each 4D-CT dataset. Five types of reference images from this stage were generated from four 4D datasets and 3D images

(FB, Aug-FB, AIP, and Mid-V images and 10 phases of 4D-CT images). All reconstructed images were subsequently sent to the Monaco Treatment Planning System using the DICOM connection protocol.

Target volume delineation

Target volume delineation was performed in a Monaco Treatment Planning System to obtain the gross tumour volume (GTV), ITV, and planning target volume (PTV) were determined for each image reference. All images were delineated at the same window level i.e., lung window. No additional margin was applied for microscopic area extension (CTV = GTV). GTV was depicted using the image threshold method, where all pixels meeting the criteria belong to the target, while those outside the criteria become the background. The GTV on Aug-FB images was delineated on all three images, and the Boolean value was determined to delineate the ITV. In 4D-CT image datasets, the ITV from 10 phases was attained from the Boolean value of all delineated GTVs on all 10 phases to obtain the ITV_{10} reference image (ITV_{10} -based). The ITV for AIP images was drawn manually and was done by one person to avoid inter-observer variability [18]. Therefore, the target volumes for all images were determined by one person to avoid variability between observers. For the Mid-V phase, the GTV was the tumour TV (target volume) [19]. Then, on ITV_{Aug-FB} , ITV_{10} , and ITV_{AIP} images, a 5-mm margin was added to establish the PTV [5, 10, 15]. PTV margins for Mid-V images were derived by adding a margin according to the simplified van Herk formula (Eq. 1) [10].

$$\text{Margin PTV} = \text{Margin without breathing} + 0.15 \times \text{range of motion}$$

where margin PTV is a margin with breathing that will be added to the TV_{mid-v} . The margin without breathing was arranged by 5-mm according to the PTV margin used in our center. Then, the range of motion is given by the amplitude of motion.

However, in the FB images, the ITV was not depicted because the images were not subjected to motion management such that from the GTV, the additional PTV margin was 10 mm. Furthermore,

treatment planning was performed at TPS Monaco for all the reference CT images that were drawn.

Planning

SBRT with a single partial anticlockwise volumetric modulated arc from 20° to 200° was planned and optimized in Monaco for delivery using 6-MV beam energy in the flattening filter-free (FFF) mode, and doses were calculated with a Monte Carlo algorithm. The planning dose in this study was 40.5 Gy in 3 fractions or 13.5 Gy per fraction, where the PTV was described as receiving 65–90% of the isodose line, and 95% of the PTV received a prescription dose ($D_{95PTV} > 40.5$ Gy) [19]. The dose in the spinal cord was maintained as low as possible with the limit not exceeding 18 Gy, and the ipsilateral lung receiving a 20-Gy dose was no more than 25% of the volume [20]. The planning parameters mentioned above were applied to all reference images. Then, for each image, optimization was carried out to obtain a dose meeting the predetermined constraints and desired dose distribution. The quality parameters of the planning results were evaluated in each plan. Furthermore, all plans were tested using Friedman's ANOVA test to determine the significance of the similarities in all plans ($p > 0.05$). When the dose measurement is carried out, the results can be compared between all the reference images.

Image registration

Image registration was carried out by aligning the CT image with the CBCT image obtained immediately before treatment was performed. The VersaHD VI system has 4D "Symmetry" and 3D "Chest" registration features, and both registration modes were utilized in this study. Registration was performed automatically using the "mask" registration feature with the Grey Value 4D (T) automatic registration algorithm method for 4D reference images and the Grey Value (T) algorithm method for 3D reference images. This procedure was performed by creating a 3D region of interest (ROI) on the desired structure and adding a 5-mm margin around it. In this case, the target volume and correction reference were located in the middle of the GTV. Table 1 summarizes the image registration pairs along with the image guide methods used. After registration was complete, the CBCT software provided position correction.

Table 1. Image registration methods between reference images and localization images

Image-guided method	Reference image	Localization image	Registration method
3D-CBCT to 3D helical	FB	3D-CBCT	Automatic
3D-CBCT to 3D helical	Aug-FB	3D-CBCT	Automatic
4D-CBCT exhale auto to exhale 4D-CT	ITV ₁₀ -based (phase 0%)	4D-CBCT	Automatic (exhalation)
AIP 4D-CBCT to AIP 4D-CT	AIP-based	4D-CBCT	Automatic (mean)
4D-CBCT to Mid-V CT	Mid-V phase	4D-CBCT	Automatic (mean)

3D — three-dimensional; 4d — four-dimensional; CBCT — cone beam computed tomography; AIP — average intensity projection; FB — free breathing; AugFB — augmentation free breathing; Mid-V — mid-ventilation phase; ITV — internal target volume

Dose delivery and evaluation

The delivery dose with SBRT was completed on a Linac Elekta VersaHD™ X-ray Volume Imager (XVI) (Elekta Ltd, Crawley West Sussex, United Kingdom). Gafchromic EBT3 film was used for dose measurement in this study. The film was cut to the size of the target diameter and placed in a coronal plane position at the centre of the acrylic tumour target surrogate. Then, after delivery, the dosimeter was read using an EPSON 10000 expression XL scanner. Next, ImageJ software was used to read the scan results of the EBT3 film.

Dose evaluation and verification were completed based on AAPM TG 119 of 2009. The dose obtained from the measurement results was compared with the planned dose for verification purposes. To calculate the amount of dose deviation ($\Delta\%$) between the measurement results (D_m) and the planned dose (D_{plan}), equation (2) was used.

$$\Delta\% = \left(\frac{D_m - D_{plan}}{D_{plan}} \right) \times 100\%$$

Results

Target delineation results

Table 2 shows the target motion along the SI direction and the delineation results for the five reference images for each variation as viewed in the frontal plane. The red, green, and blue contours represent the GTV, ITV, and PTV, respectively.

Target volume evaluation

As depicted on the graph in Figure 2, the FB and Aug-FB images do not provide GTV values that are close to the original target volume. The GTVs obtained for a target of either 2 cm or 3 cm in diameter are smaller than the GTV calculated mathematically and the GTV on a static image.

These results are consistent with research conducted by Mohatt et al. [15] in 2017, which showed that a longer amplitude of breathing within the same breathing period corresponded to a blurrier image and a smaller depicted GTV.

Meanwhile, ITV₁₀-based images and images in the mid-ventilation phase provided volume values identical to the target volume calculated mathematically for both motion targets with amplitudes of 5 mm and 10 mm, which were 4.2 cm³ for the 2-cm target and 14.2 cm³ for the 3-cm target.

The ITV for Aug-FB images was identical to the volume calculated mathematically. The ITV_{Aug-FB} values for the 2-cm target with 5-mm and 10-mm movement were 5.80 cm³ and 7.30 cm³, respectively, and those for the 3-cm target with 5-mm and 10-mm movement were 17.60 cm³ and 20.90 cm³, respectively. These values can be recommended to hospitals that do not yet have 4D-CT, as stated by Mohatt et al. [15] based on their research, where Aug-FB images had identical performance to ITV₁₀ images obtained from 10 phases of a 4D-CT dataset.

The PTVs from ITV₁₀-based, AIP, and Mid-V images were smaller than the PTVs from images acquired with the 3D protocol (FB and FB-aug). The percentage of PTV reduction with the application of 4D-CT ranged from 21.21% to 48.70% of the PTV FB image, a 3D image acquired without motion management, while the percentage of PTV reduction ranged from 2.96% to 13.19% of the PTV Aug-FB image, a 3D image with motion management.

Planning evaluation and Friedman’s ANOVA test

The results in Table 3 show that the maximum dose value does not exceed the upper limit of the dose prescribed, namely, the 65% isodose line or

Table 2. Target volume delineation results. FB — free breathing; AugFB — augmentation free breathing; AIP — average intensity projection; ITV — internal target volume; Mid-V — mid-ventilation phase

Reference images	Target 2 cm		Target 3 cm	
	5 mm	10 mm	5 mm	10 mm
Static				
FB				
Aug-Fb				
AIP				
ITV ₁₀				
Mid-V				

6230.77 cGy, and yields an average prescription dose coverage of approximately 99.56% on the PTV. For the conformity index (CI), only ITV₁₀ and Mid-V images fall into the minor deviation category according to RTOG-0915, and for intermediate dose spillage (R_{50%}), almost all planning values fall into the minor deviation category.

Table 4 shows the results of Friedman’s ANOVA test, which is based on the p-value or significant value of the planning achievement parameters in the target. Several data comparisons were performed: the average dose (D_{mean}) of the PTV, monitor units (MU), prescription dose coverage, the CI, and R_{50%}. The results of the Friedman’s ANOVA test for all these parameters (D_{mean} PTV, MU, Coverage, CI and R_{50%}) showed no significant differences between all plans carried out on all reference images with 5% error is given (p > 0.05).

Results of position off-set after registration

As shown in Table 5, for moving targets, the AIP image has the smallest position correction, with correction values in the lateral, longitudinal, and vertical directions below ± 2 mm. Meanwhile, the largest correction is evident in the FB image, which has a position correction greater than ± 2 mm in the longitudinal direction for a target with a diameter of 3 cm.

Dose evaluation

Table 6 shows the deviations between the planned doses and measured doses. The first deviation refers to the measured dose compared to the mean dose of the ROI GTV on the centre of a caudal plane in the Monaco Treatment Planning System. The second deviation represents a comparison to the ROI

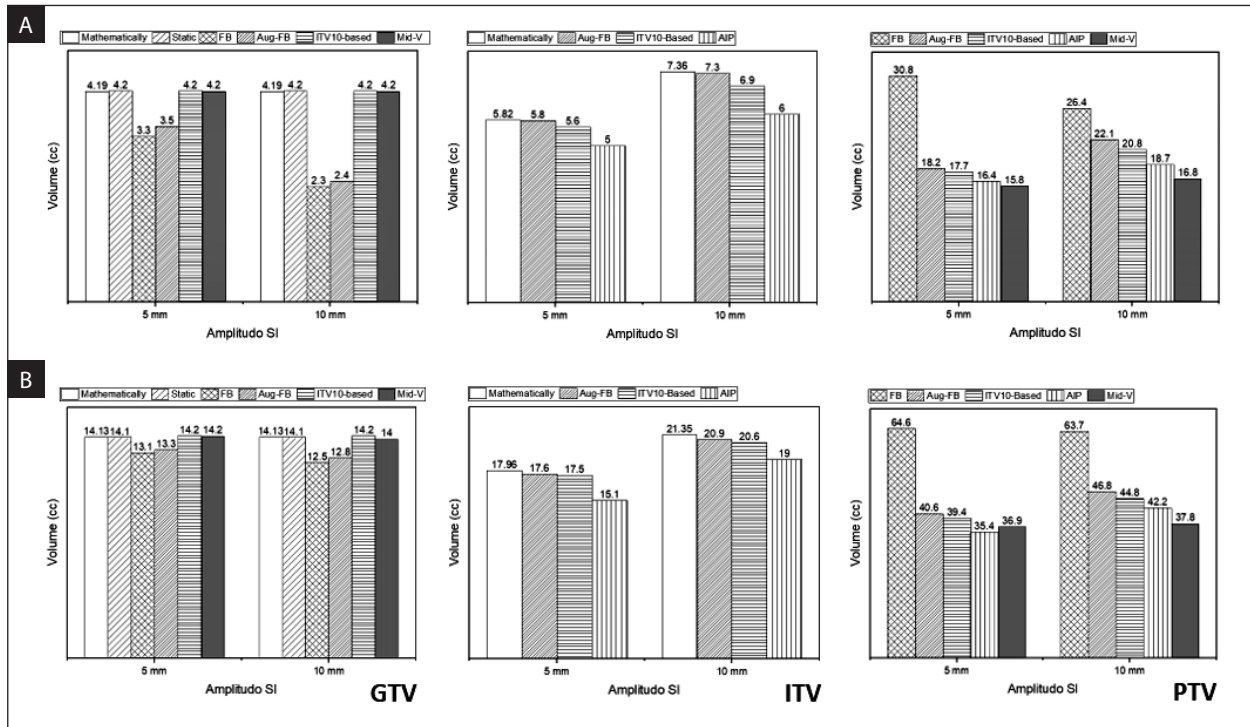


Figure 2. Comparison of gross tumour volumes (GTVs), internal target volumes (ITVs), and planning target volumes (PTVs) (in cm³) on several reference images for a (A) 2-cm-diameter target and (B) 3-cm-diameter target

Table 3. Results of planning achievements

Reference images	Mean Dose (cGy)	Max Dose (cGy)	Plan quality parameters		
			Coverage (%)	CI	R _{50%}
Static	4823.4 ± 149.3	5954.35 ± 242.0	99.1 ± 0.25	1.14 ± 0.01	5.04 ± 0.40
FB	4878.1 ± 134.4	5864.85 ± 282.5	99.2 ± 0.81	1.15 ± 0.06	5.04 ± 0.58
Aug-FB	4939.2 ± 142.2	5837.3 ± 213.4	99.7 ± 0.09	1.16 ± 0.04	5.25 ± 0.53
ITV ₁₀	5005.8 ± 107.4	5912.0 ± 177.0	99.8 ± 0.09	1.24 ± 0.09	5.22 ± 0.86
AIP	5045.2 ± 75.8	5980.9 ± 79.8	99.6 ± 0.32	1.20 ± 0.10	5.38 ± 0.77
Mid-V	4951.2 ± 126.5	5895.6 ± 122.2	98.1 ± 0.72	1.12 ± 0.08	5.13 ± 0.73

CI — conformity index; FB — free breathing; AugFB — augmentation free breathing; ITV — internal target volume; AIP — average intensity projection; Mid-V — mid-ventilation phase

Table 4. Results of Friedman’s ANOVA test

Parameter	p-value
D _{mean} PTV	0.470
MU	0.921
Coverage	0.154
CI	0.434
R _{50%}	0.591

D_{mean} — average dose; PTV — planning target volume; MU — monitor unit; CI — conformity index; R_{50%} — intermediate dose spillage

on the centre of the GTV (< 3% of the first ROI) [21]. The largest deviation occurs in the FB image

for a target with a diameter of 3 cm and a motion amplitude of 10 mm, reaching 10.39%.

The FB image had the largest deviation for a 3-cm target and a motion amplitude of 10 mm, reaching 10.39%. Similarly, the deviation was 9.21% for the Aug-FB image with a 3-cm target and a motion amplitude of 10 mm. The deviations for the 3-cm and 2-cm static targets were 5.73% and 5.17%, respectively, while the deviation obtained from the reference image obtained by the 4D method was in the range of 5.1% to 7.28%. A decrease in the discrepancy was observed in this second comparison, which was close to zero in several reference images.

Table 5. Position correction after registration with localized images

Reference Images	Variations	Position off-set [mm]		
		Lat (x)	Long (y)	Vert (z)
Static	3 cm	0.10	0.40	0.10
	2 cm	0.06	0.16	-0.10
FB	1	0.04	-0.24	0.08
	2	0.00	-0.28	-0.10
	3	0.01	0.08	-0.12
	4	0.25	0.26	-0.19
Aug-FB	1	0.15	-0.05	-0.05
	2	0.18	0.02	-0.21
	3	0.10	0.06	-0.19
	4	0.11	0.05	-0.19
ITV ₁₀	1	-0.19	0.07	-0.27
	2	-0.01	-0.24	0.03
	3	-0.28	0.05	-0.15
	4	0.00	-0.24	-0.19
AIP	1	-0.18	0.16	-0.16
	2	0.00	-0.12	-0.02
	3	-0.17	0.13	-0.09
	4	-0.13	0.02	-0.13
Mid-V	1	-0.12	0.00	-0.19
	2	0.02	-0.16	0.03
	3	-0.26	-0.05	-0.29
	4	-0.04	-0.07	-0.16

*note: code 1 refers to variation for a 3 cm target with 10-mm amplitude in the SI direction; code 2, a 3-cm target with 5-mm amplitude; code 3, a 2-cm target with 10-mm amplitude; and code 4, a 2-cm target with 5-mm amplitude. FB — free breathing; AugFB — augmentation free breathing; ITV — internal target volume; AIP — average intensity projection; Mid-V — mid-ventilation phase

Table 6. Deviations between the planned and measured doses for all reference images

Reference images	Variations	Deviation (%)	
		Mean GTV (ROI on the centre of the caudal plane)	ROI on the centre of the GTV (< 3% of the first ROI)
Static	3 cm	5.73	0.96
	2 cm	5.17	-0.16
FB	1	10.39	1.14
	2	5.19	-2.11
	3	4.21	-0.34
	4	4.05	-0.19
Aug-FB	1	9.21	2.76
	2	4.43	-0.69
	3	2.87	-2.31
	4	4.60	-1.30
ITV ₁₀	1	5.10	-1.77
	2	5.62	2.19
	3	7.00	2.53
	4	6.92	2.33
AIP	1	6.74	1.67
	2	6.84	2.15
	3	7.28	0.09
	4	7.09	0.10
Mid-V	1	6.63	0.80
	2	6.75	2.73
	3	5.82	1.49
	4	3.58	2.80

GTV — gross tumour volume; ROI — region of interest; FB — free breathing; AugFB — augmentation free breathing; ITV — internal target volume; AIP — average intensity projection; Mid-V — mid-ventilation phase

Discussion

In the target volume evaluation depicted in Figure 2, the GTV obtained from images acquired from 4D-CT datasets had the same value as the static or mathematically calculated GTV because the ITV₁₀-based approach will depict the target image in all phases of the reconstruction. Similarly, when delineating the target, the Mid-V step can be helpful since the Mid-V image represents a single phase of the 10 phases of the 4D-CT dataset obtained by examining the location of the tumour during respiration closest to the time-weighted mean position [10].

Meanwhile, in ITV comparisons, reference images reconstructed from 4D-CT datasets had smaller ITVs than 3D-CT reference images. This decrease in ITV will be reflected in the greater benefit to

organs at risk after the PTV margin has been added without reducing the movement target area. The smallest reduction in the target volume achieved in the case of lung cancer will cause a difference in proper preparation of radiation therapy and prevent immediate and slow effects on normal tissue around the tumour. When irradiation is administered, a decrease in the PTV can be interpreted as less normal tissue exposed to high doses of radiation, which can decrease toxicity. Moreover, this modality is very useful for limiting the size of the PTV for larger tumours [10]. Thus, an increase in the number of patients qualifying for SBRT who could have been denied because of normal tissue constraints is another possible benefit of reducing the PTV [22].

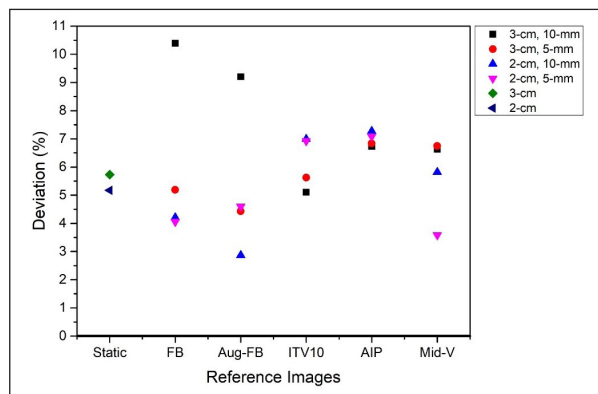


Figure 3. The distribution of discrepancies in all reference images for the first comparison. FB — free breathing; AugFB — augmentation free breathing; ITV — internal target volume; AIP — average intensity projection; Mid-V — mid-ventilation phase

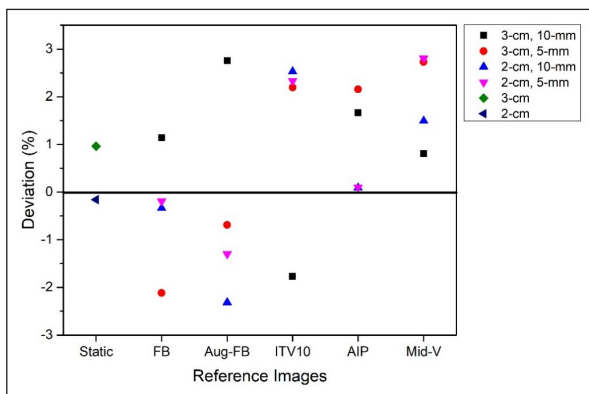


Figure 4. The distribution of discrepancies in all reference images in the second comparison. FB — free breathing; AugFB — augmentation free breathing; ITV — internal target volume; AIP — average intensity projection; Mid-V — mid-ventilation phase

To increase self-confidence when conducting SBRT, the position must be corrected immediately before treatment using localized imagery (CBCT). In the symmetry protocol, target positions are identified in each phase of 4D-CBCT breathing. The difference in the target position on the reference images relative to the target position in each CBCT phase and then the position error at each position in the 10 CBCT phases are calculated such that the average value is the correction of the phantom position [23].

Table 6 shows the deviation from the ratio between the planned doses and measured doses. This deviation occurs for several reasons, including target movement, which occurs not only in the SI direction but also with an angle of motion of 8°, causing the target to move incorrectly in line with the direction of MLC movement. As reported in a study by Court et al. [24], tumours that constantly move parallel or perpendicular to MLC leaf movement can cause a 10% greater difference in dose delivery. In another study, Court et al. [25] also reported that a large amplitude of motion and a long period of tumour motion can cause a large difference in the discrepancy of the target. In addition, the use of the FB SBRT technique is also one of the reasons to increase the dose to the GTV. Smith et al. [26] stated that VMAT and FFF with the FB SBRT technique yielded discrepancy results identical to the discrepancy values in this study, which were 5.0% for static targets and 7.4% for moving targets. Therefore, further research applying motion management during treatment is necessary, namely, the gating or tracking technique.

A decrease in the discrepancy value was observed in this second comparison. The reduction obtained was close to zero in some reference images, which is in line with the results of Ong et al. [21], who observed a small area in the middle of the target, namely, a decrease in discrepancy to < 4%. The measured dose did not exceed the prescription dose of the 65% isodose line and was not less than the 90% isodose line. The use of VMAT and FFF in the SBRT technique with the 4D image-guided method can reduce the risk of either underdose or overdose due to target movement. The distributions of discrepancy values can be viewed in Figure 3 for the first comparison and Figure 4 for the second comparison.

Some drawbacks of phantom studies compared to clinical cases must be discussed. First, the time and amplitude of tumour movement in the phantom were clear. Second, the tumour travelled only around two axes within the phantom. Finally, the phantom tumour was non-deformable and rigid. Irregular breathing patterns, 3D motion, and tumour deformation introduce additional errors concerning actual patient situations, which experimentally reflect the upper limits of what can be considered the best-case scenario [15].

Conclusions

The 4D-CT modality can reduce the PTV without reducing target coverage by 29.17% to 48.70% such that less normal tissue is exposed to high doses of radiation with irradiation treatment, which can

potentially reduce toxicity. The greatest discrepancy in this value may be due to the large amplitude of motion and the long period of tumour motion, which will cause a large difference in the discrepancy of the target. However, the measured dose did not exceed or drop below the prescription dose.

Conflict of interest

The authors declare that they have no conflicts of interest.

Funding

This research was supported by a PUTI grant under contract number NKB-2411/UN2.RST/HKP.05.00/2020 from the University of Indonesia.

Acknowledgement

The authors thank the management and all staff members in the Department of Radiotherapy, Cipto Mangunkusumo Hospitals.

References

- Stevens CW, Munden RF, Forster KM, et al. Respiratory-driven lung tumor motion is independent of tumor size, tumor location, and pulmonary function. *Int J Radiat Oncol Biol Phys.* 2001; 51(1): 62–68, doi: [10.1016/s0360-3016\(01\)01621-2](https://doi.org/10.1016/s0360-3016(01)01621-2), indexed in Pubmed: [11516852](https://pubmed.ncbi.nlm.nih.gov/11516852/).
- Huang CY, Tehrani JN, Ng JA, et al. Six degrees-of-freedom prostate and lung tumor motion measurements using kilovoltage intrafraction monitoring. *Int J Radiat Oncol Biol Phys.* 2015; 91(2): 368–375, doi: [10.1016/j.ijrobp.2014.09.040](https://doi.org/10.1016/j.ijrobp.2014.09.040), indexed in Pubmed: [25445555](https://pubmed.ncbi.nlm.nih.gov/25445555/).
- Sweeney RA, Seubert B, Stark S, et al. Accuracy and inter-observer variability of 3D versus 4D cone-beam CT based image-guidance in SBRT for lung tumors. *Radiat Oncol.* 2012; 7: 81, doi: [10.1186/1748-717X-7-81](https://doi.org/10.1186/1748-717X-7-81), indexed in Pubmed: [22682767](https://pubmed.ncbi.nlm.nih.gov/22682767/).
- Landberg T, Chavaudra J, Dobbs J, et al. Report 62. *J Int Comm Radiat Units Meas.* 2016; os32(1), doi: [10.1093/jicru/os32.1.report62](https://doi.org/10.1093/jicru/os32.1.report62).
- Khamfongkhrua C, Thongsawad S, Tannanonta C, et al. Comparison of CT images with average intensity projection, free breathing, and mid-ventilation for dose calculation in lung cancer. *J Appl Clin Med Phys.* 2017; 18(2): 26–36, doi: [10.1002/acm2.12037](https://doi.org/10.1002/acm2.12037), indexed in Pubmed: [28300381](https://pubmed.ncbi.nlm.nih.gov/28300381/).
- Richter A, Wilbert J, Baier K, et al. Feasibility study for markerless tracking of lung tumors in stereotactic body radiotherapy. *Int J Radiat Oncol Biol Phys.* 2010; 78(2): 618–627, doi: [10.1016/j.ijrobp.2009.11.028](https://doi.org/10.1016/j.ijrobp.2009.11.028), indexed in Pubmed: [20452143](https://pubmed.ncbi.nlm.nih.gov/20452143/).
- Korreman S, Persson G, Nygaard D, et al. Respiration-correlated image guidance is the most important radiotherapy motion management strategy for most lung cancer patients. *Int J Radiat Oncol Biol Phys.* 2012; 83(4): 1338–1343, doi: [10.1016/j.ijrobp.2011.09.010](https://doi.org/10.1016/j.ijrobp.2011.09.010), indexed in Pubmed: [22245194](https://pubmed.ncbi.nlm.nih.gov/22245194/).
- Allen AM, Siracuse KM, Hayman JA, et al. Evaluation of the influence of breathing on the movement and modeling of lung tumors. *Int J Radiat Oncol Biol Phys.* 2004; 58(4): 1251–1257, doi: [10.1016/j.ijrobp.2003.09.081](https://doi.org/10.1016/j.ijrobp.2003.09.081), indexed in Pubmed: [15001270](https://pubmed.ncbi.nlm.nih.gov/15001270/).
- Nakamura M, Narita Y, Matsuo Y, et al. Geometrical differences in target volumes between slow CT and 4D CT imaging in stereotactic body radiotherapy for lung tumors in the upper and middle lobe. *Med Phys.* 2008; 35(9): 4142–4148, doi: [10.1118/1.2968096](https://doi.org/10.1118/1.2968096), indexed in Pubmed: [18841867](https://pubmed.ncbi.nlm.nih.gov/18841867/).
- Thomas SJ, Evans BJ, Harihar L, et al. An evaluation of the mid-ventilation method for the planning of stereotactic lung plans. *Radiother Oncol.* 2019; 137: 110–116, doi: [10.1016/j.radonc.2019.04.031](https://doi.org/10.1016/j.radonc.2019.04.031), indexed in Pubmed: [31085390](https://pubmed.ncbi.nlm.nih.gov/31085390/).
- Huang L, Park K, Boike T, et al. A study on the dosimetric accuracy of treatment planning for stereotactic body radiation therapy of lung cancer using average and maximum intensity projection images. *Radiother Oncol.* 2010; 96(1): 48–54, doi: [10.1016/j.radonc.2010.04.003](https://doi.org/10.1016/j.radonc.2010.04.003), indexed in Pubmed: [20430460](https://pubmed.ncbi.nlm.nih.gov/20430460/).
- Hugo GD, Liang J, Campbell J, et al. On-line target position localization in the presence of respiration: a comparison of two methods. *Int J Radiat Oncol Biol Phys.* 2007; 69(5): 1634–1641, doi: [10.1016/j.ijrobp.2007.08.023](https://doi.org/10.1016/j.ijrobp.2007.08.023), indexed in Pubmed: [18029112](https://pubmed.ncbi.nlm.nih.gov/18029112/).
- Shin HJ, Kim SW, Kay C, et al. Evaluation of the Elekta Symmetry™ 4D IGRT system by using a moving lung phantom. *Journal of the Korean Physical Society.* 2015; 67(1): 260–263, doi: [10.3938/jkps.67.260](https://doi.org/10.3938/jkps.67.260).
- Yin FF, Wong J, Balter J, et al. The Role of In-Room kV X-Ray Imaging for Patient Setup and Target Localization. Report of AAPM Task Group 104. Data Management. 2009, doi: [10.37206/104](https://doi.org/10.37206/104).
- Mohatt DJ, Keim JM, Greene MC, et al. An investigation into the range dependence of target delineation strategies for stereotactic lung radiotherapy. *Radiat Oncol.* 2017; 12(1): 166, doi: [10.1186/s13014-017-0907-8](https://doi.org/10.1186/s13014-017-0907-8), indexed in Pubmed: [29100548](https://pubmed.ncbi.nlm.nih.gov/29100548/).
- Dai Z, Zhang H, Xie Y, et al. Validation of Geometric and Dosimetric Accuracy of Edge Accelerator Gating With Electromagnetic Tracking: A Phantom Study. *IEEE Access.* 2019; 7: 127693–127702, doi: [10.1109/access.2019.2934858](https://doi.org/10.1109/access.2019.2934858).
- Clinical Methods: The History, Physical, and Laboratory Examinations. In: Billelt HH. ed. *Anesthesiology* 3rd ed. 1967.
- Borm KJ, Oechsner M, Wiegandt M, et al. Moving targets in 4D-CTs versus MIP and AIP: comparison of patients data to phantom data. *BMC Cancer.* 2018; 18(1): 760, doi: [10.1186/s12885-018-4647-4](https://doi.org/10.1186/s12885-018-4647-4), indexed in Pubmed: [30041618](https://pubmed.ncbi.nlm.nih.gov/30041618/).
- Ehrbar S, Jöhl A, Tartas A, et al. ITV, mid-ventilation, gating or couch tracking - A comparison of respiratory motion-management techniques based on 4D dose calculations. *Radiother Oncol.* 2017; 124(1): 80–88, doi: [10.1016/j.radonc.2017.05.016](https://doi.org/10.1016/j.radonc.2017.05.016), indexed in Pubmed: [28587761](https://pubmed.ncbi.nlm.nih.gov/28587761/).
- Mutter RW, Liu F, Abreu A, et al. Dose-volume parameters predict for the development of chest wall pain after stereotactic body radiation for lung cancer. *Int J Radiat Oncol Biol Phys.* 2012; 82(5): 1783–1790, doi: [10.1016/j.ijrobp.2011.03.053](https://doi.org/10.1016/j.ijrobp.2011.03.053), indexed in Pubmed: [21868173](https://pubmed.ncbi.nlm.nih.gov/21868173/).
- Ong CL, Dahele M, Slotman BJ, et al. Dosimetric impact of the interplay effect during stereotactic lung radiation therapy delivery using flattening filter-free

- beams and volumetric modulated arc therapy. *Int J Radiat Oncol Biol Phys.* 2013; 86(4): 743–748, doi: [10.1016/j.ijrobp.2013.03.038](https://doi.org/10.1016/j.ijrobp.2013.03.038), indexed in Pubmed: [23773394](https://pubmed.ncbi.nlm.nih.gov/23773394/).
22. Peulen H, Belderbos J, Rossi M, et al. Mid-ventilation based PTV margins in Stereotactic Body Radiotherapy (SBRT): a clinical evaluation. *Radiother Oncol.* 2014; 110(3): 511–516, doi: [10.1016/j.radonc.2014.01.010](https://doi.org/10.1016/j.radonc.2014.01.010), indexed in Pubmed: [24560765](https://pubmed.ncbi.nlm.nih.gov/24560765/).
23. Li J, Harrison A, Yu Y, et al. Evaluation of Elekta 4D cone beam CT-based automatic image registration for radiation treatment of lung cancer. *Br J Radiol.* 2015; 88(1053): 20140620, doi: [10.1259/bjr.20140620](https://doi.org/10.1259/bjr.20140620), indexed in Pubmed: [26183932](https://pubmed.ncbi.nlm.nih.gov/26183932/).
24. Court LE, Wagar M, Ionascu D, et al. Management of the interplay effect when using dynamic MLC sequences to treat moving targets. *Med Phys.* 2008; 35(5): 1926–1931, doi: [10.1118/1.2896083](https://doi.org/10.1118/1.2896083), indexed in Pubmed: [18561668](https://pubmed.ncbi.nlm.nih.gov/18561668/).
25. Court L, Wagar M, Bogdanov M, et al. Use of reduced dose rate when treating moving tumors using dynamic IMRT. *J Appl Clin Med Phys.* 2010; 12(1): 3276, doi: [10.1120/jacmp.v12i1.3276](https://doi.org/10.1120/jacmp.v12i1.3276), indexed in Pubmed: [21330973](https://pubmed.ncbi.nlm.nih.gov/21330973/).
26. Smith AG, Serago C, Hintenlang K, et al. Dosimetric evaluation of the interplay effect for non-respiratory-gated VMAT treatment of moving targets with high dose rate FFF beams. *IFMBE Proceedings.* 2015: 444–447, doi: [10.1007/978-3-319-19387-8_108](https://doi.org/10.1007/978-3-319-19387-8_108).